Published in final edited form as:
Dev Biol. 2006 October 1; 298(1): 59–70.

Genetic interactions between *Drosophila melanogaster* menin and Jun/Fos

Aniello Cerrato[a,*], **Michael Parisi**[a], **Sonia Santa Anna**[b], **Fanis Missirlis**[c], **Siradanahalli Guru**[b,1], **Sunita Agarwal**[a], **David Sturgill**[a], **Thomas Talbot**[d], **Allen Spiegel**[a], **Francis Collins**[b], **Settara Chandrasekharappa**[b], **Stephen Marx**[a], and **Brian Oliver**[a]

a *National Institute of Diabetes and Digestive and Kidney Diseases, Department of Health and Human Services, Bethesda, MD 20892, USA*

b *National Human Genome Research Institute, Department of Health and Human Services, Bethesda, MD 20892, USA*

c *National Institute of Child Health and Human Development, Department of Health and Human Services, Bethesda, MD 20892, USA*

d *Office of the Director, National Institutes of Health, Department of Health and Human Services, Bethesda, MD 20892, USA*

Abstract

Menin is a tumor suppressor required to prevent multiple endocrine neoplasia in humans. Mammalian menin protein is associated with chromatin modifying complexes and has been shown to bind a number of nuclear proteins, including the transcription factor JunD. Menin shows bidirectional effects acting positively on c-Jun and negatively on JunD. We have produced protein null alleles of *Drosophila menin* (*mnn1*) and have over expressed the Mnn1 protein. Flies homozygous for protein-null *mnn1* alleles are viable and fertile. Localized over-expression of Mnn1 causes defects in thoracic closure, a phenotype that sometimes results from insufficient Jun activity. We observed complex genetic interactions between *mnn1* and *jun* in different developmental settings. Our data support the idea that one function of menin is to modulate Jun activity in a manner dependent on the cellular context.

Keywords

AP1; Oxidative stress; Paraquat; Life span; Cleft thorax; Tumor suppressor; Multiple endocrine neoplasia type I

Introduction

Human multiple endocrine neoplasia type 1 (MEN1) is an autosomal dominant cancer syndrome characterized by tumors occurring prevalently in endocrine tissues. Common features of most MEN1 tumors are low proliferation rates, well-differentiated morphology and excessive hormone secretion. Hereditary tumors arise in individuals heterozygous for a loss-of-function *MEN1* allele followed by somatic loss of wild type alleles. Sporadic tumors also show bi-allelic loss of *MEN1* (Agarwal et al., 2004). The *MEN1* locus encodes menin, a nuclear

* Corresponding author. Istituto di Endocrinologia ed Oncologia Sperimentale/CNR, c/o Dipartimento di Biologia e Patologia Cellulare e Molecolare, Universita' di Napoli "Federico II", Via S. Pansini, 5, 80131 Napoli, Italy. Fax: +39 0817463037. E-mail address: a.cerrato@sun.ceos.na.cnr.it (A. Cerrato).
[1]Current address: Pfizer Global Research and Development, Ann Arbor, MI, USA.

protein with two nuclear-localization sites at the C-terminal quarter of the protein, but no other overt sequence motifs (Chandrasekharappa et al., 1997; Guru et al., 1998). Menin is ubiquitously expressed, but only shows a loss of heterozygosity phenotype in a highly restricted set of cells (Scacheri et al., 2004). This context dependency suggests that regulated co-factors or modifiers act in conjunction with menin for cell-type specific function. Menin has also been found in a SET1-like histone methylation complex (Hughes et al., 2004; Karnik et al., 2005; Milne et al., 2005; Yokoyama et al., 2004, 2005). The mouse *menin* gene is required for embryonic viability and, like in humans, inactivation of both alleles results in endocrine tumors (Crabtree et al., 2001, 2003). Therefore, menin is a classic tumor suppressor in the endocrine system. Interestingly, there is also recent evidence that menin is an oncogenic co-factor in Mixed Lineage Leukemia (Yokoyama et al., 2005). The nature of this dual growth suppressing and enhancing role in the regulation of proper cell number and differentiation has not been clarified.

Multiple potential transcription factor partners for mammalian menin protein have been identified (Agarwal et al., 2004) including JunD, which has been shown to interact directly with menin (Agarwal et al., 1999). It is unclear how these protein–protein interactions relate to menin in the SET-1 like histone methylation complex, although it is possible that menin association with many different nuclear proteins helps target the complex to appropriate regions of chromatin. Experiments performed in immortalized mouse embryo fibroblasts have shown that menin binding to JunD is necessary for JunD to act as a growth suppressor (Agarwal et al., 2003). Menin functions to reduce JunD activity (Agarwal et al., 1999; Gobl et al., 1999; Kim et al., 2005; Naito et al., 2005) and has been shown to inhibit the accumulation of active phosphorylated JunD or c-Jun (Gallo et al., 2002). Even though menin does not directly bind c-Jun, it augments the transcriptional activity of this transcriptional factor (Knapp et al., 2000). Thus, menin is strongly implicated in regulating Jun function. Interestingly, according to the potential roles of menin to promote or suppress tumorigenesis, menin can act in turn negatively on JunD or positively on c-Jun function.

Jun and Fos heterodimers are well-known regulators of tumorigenesis, differentiation, apoptosis, immune and stress responses in both vertebrates and Drosophila (Kockel et al., 2001; Mechta-Grigoriou et al., 2001). There are a number of mammalian homodimers and heterodimers consisting in c-Jun, JunB or JunD and c-Fos, FosB, Fra1 or Fra2 combinations (Mechta-Grigoriou et al., 2001). Unlike mammals, *Drosophila* has a single Jun and a single Fos (Kockel et al., 2001). *Drosophila* Jun has features of both JunD and c-Jun. This makes *Drosophila* a good reductionist model for learning more about Jun/menin interactions. While experiments to see if *Drosophila* menin binds Jun have been negative (Guru et al., 2001), genetic interactions have not been explored. In this study, we have specifically investigated the functional connection between *Drosophila* menin and Jun.

The *Drosophila melanogaster* menin protein (Mnn1) is 47% identical to the human protein, including 69% of the amino acid residues that are required for tumor suppression in human endocrine tissues (Guru et al., 2001; Maruyama et al., 2000). The ongoing sequencing of multiple species in *Drosophila* reveals that menin is highly conserved among them (Fig. 1). Despite this high degree of conservation, menin is not required for viability in *D. melanogaster*. Flies lacking *mnn1* expression are viable and fertile (Busygina et al., 2004; Papaconstantinou et al., 2005). One report suggests that *mnn1* is required for a wild type life span and some aspect of either chromosome stability or DNA repair (Busygina et al., 2004), while another report suggests that *mnn1* is required for a robust response to various types of stress (Papaconstantinou et al., 2005).

We have isolated two protein-null *mnn1* alleles and have generated transgenic flies for the controlled over-expression of *Drosophila* Mnn1 protein. As previously reported, *mnn1*$^{-}$

Drosophila is viable and fertile. It has been reported that uniform over-expression of *mnn1* has no effect on development or viability in flies (Papaconstantinou et al., 2005). We find that over-expression results in pharate-adult phenotype, proboscis ablation and a cleft thorax. These over-expression phenotypes are modified by both gain-of-function and loss-of-function alleles of *jun*. Dominant-negative alleles of *fos* are enhanced by loss-of-function alleles of *mnn1*. The finding that both *Drosophila* and mammalian menin (Agarwal et al., 1999, 2003) are capable of interacting with Jun suggests that an evolutionarily conserved menin function in normal development and disease is linked to the Jun/Fos family of transcriptional regulators. Interestingly, as in mammals, *Drosophila* menin shows bidirectional modulation of Jun function.

Materials and methods

Flies

A P-element insertion at the *mnn1* locus, $P\{wHy\}^{30G01}$ (Huet et al., 2002), is located in the 5′ untranslated region (at + 601 bp from transcription start, 503 bp upstream of the start codon) of the gene models based on two studies directed at *mnn1* characterization (Guru et al., 2001; Maruyama et al., 2000). We have not found evidence to support the slightly different gene models annotated at FlyBase (FlyBase, 2003). Imprecise excision alleles were generated by crossing $P\{wHy\}^{30G01}$ to $\Delta 2\text{–}3$ flies. We screened 14,984 chromosomes identifying $y^- w^+$ lines (159) and $w^- y^-$ lines (141). Excision rearrangements were detected by Southern blots, diagnostic PCR reactions and DNA sequencing. We obtained 14 lines with rearrangements in *mnn1* DNA sequences and 12 precise-excision alleles. Two of the precise-excision lines were saved and used as isogenic controls. The $mnn1^{\Delta 46}$ allele has a deletion of 573 bp of the *mnn1* gene and the entire $P\{wHy\}^{30G01}$ insertion. This allele is missing 70 bp downstream of the first ATG of the *mnn1* ORF. The $mnn1^{\Delta 79}$ allele has a more extensive deletion of 186 bp downstream of the start codon of *mnn1*, but retains part of the 5′ sequence of $P\{wHy\}^{30G01}$ (and is w^+). The final new aberration, *Df(2L)mnn1*, is a large deficiency removing several vital genes proximal to *mnn1* (Fig. 2).

UAS-*mnn1* transgenes were generated by subcloning the full-length *Drosophila mnn1* cDNA (Guru et al., 2001) into the pUAST vector (Brand and Perrimon, 1993). Flies were transformed using standard techniques (Rubin and Spradling, 1982). Induction of *mnn1* with assorted drivers was verified by Western blotting or immunostaining with anti-Mnn1. All six *UAS-mnn1* transgenic lines showed similar results. In some cases (as noted in the text), crosses showing a strong phenotype were retested at 18°, 25° and 29°C to allow us to look for effects of different levels of Gal4 activity.

Flies were grown on GIF medium, under uncrowded conditions, at 25°C (KD Medical, Columbia MD). Extensive descriptions of mutant and *GAL4* lines can be found at FlyBase (FlyBase, 2003).

RT-PCR

RT-PCR reactions were performed on flies homozygous for *mnn1* alleles. Total RNAwas isolated from 50 homozygous female flies, aged 3–5 days and fed overnight on yeast paste. Females were chosen to increase the probability of detecting both zygotic and maternally loaded *mnn1* transcripts. Total RNA was isolated with Trizol reagent (Invitrogen, Carlsbad CA). Approximately 250 μg of total RNA was treated with 10U RQ1 DNAse (Promega, Madison WI) at 37°C, for 15 min followed by two phenol extractions and ethanol precipitation. Total RNA (25 μg) was used for first strand synthesis using 2 μg dT16–18 and three different concentrations of random hexamers that ranged to 100-fold dilutions. RNA/primers were heated 70°C for 3 min and DNA synthesis was done with Superscript according to manufacturer

protocols (Invitrogen, Carlsbad CA). Thirty cycle PCRs were done using a PTC-225 gradient thermocycler (Bio-Rad, Hercules CA).

Forward primer 5′TGTCCACGATTACCAGAAGCG overlapping the ATG sequence was designed in pair with a reverse primer 5′AGCGAGTTCCAGATCACATCCG designed in a retained sequence of exon 3 of *mnn1*; forward primer 5′TACGACATTAGGTCCCAGGTGG and reverse primer 5′TTGCTTGTGGTTGTTGCGTTAG were designed to amplify sequence spanning intron 4.

Additional primer sequences used for transcript analysis are available upon request.

Immunoblotting and microscopy

Rabbit polyclonal anti-Mnn1 was produced using a 23 a.a. peptide, LPEDLEAEQAKAELARAEQEAKE, corresponding to a.a. 464–487 as an antigen (BioCon, Bangalore India). Antiserum was affinity purified on the peptide as described (Goldsmith et al., 1987). Whole flies or tissues were directly homogenized in Laemmli buffer and separated by 8% SDS-PAGE. Blots were developed with Enhanced Chemiluminescence (Amersham, Piscataway NJ). For cell staining, tissues were dissected in PBS buffer, fixed in 2% paraformaldehyde in PBS, permeabilized in PBS with 0.1% Triton X-100, blocked in PBS with 0.1% Triton X-100 and 0.5% BSA for 2 h and incubated in rabbit anti-Mnn1 or anti-Actin (Sigma-Aldrich, St. Louis MO) overnight. After rinsing in TBS, tissues were incubated with a secondary antibody conjugated to fluorescein or rhodamine (Jackson ImmunoResearch Laboratory, West Grove PA), rinsed in TBS, counterstained with DAPI (Invitrogen, Carlsbad CA), mounted in 70% glycerol containing 2.5% DABCO (Sigma-Aldrich, St. Louis MO) and observed on a Zeiss confocal microscope.

For scanning electron microscopy, flies were fixed in 4% glutaraldehyde in PBS for 2 h at room temperature, then washed in PBS and dehydrated in a graded series of acetone-PBS (50, 70 and 100%) at room temperature. Afterwards, the specimens were critical point dried, mounted in stubs head up, sputter coated, scanned at 200, 1000 and 2500 × and photographed in a Zeiss scanning electron microscope.

Life span and paraquat resistance determinations

For life span and paraquat experiments, 0–2 day post-eclosion progeny were collected and were allowed to mate freely for 3 days. Sexes were then separated and used in the two assays. For paraquat treatments, 10 mM paraquat (Sigma-Aldrich, St. Louis MO) solution was freshly prepared in 1% sucrose. 400 μL was used to saturate two filter paper disks (Whatman, Florham Park NJ) in an otherwise empty vial. 100 flies/genotype were starved for 2 h and then transferred in groups of 20 to the disk-containing vials. Flies immediately started feeding on the sucrose-paraquat solution and their viability was scored at 5 h intervals. The experiment was performed on both sexes and repeated three times giving similar results each time. Life span determination was examined using 50 males/genotype. Flies were separated in two groups of 25 flies and placed on fresh vials of standard food every second day (starting at day 5). Replicate life span determinations were performed. Data are not pooled in the results shown. *Mnn1* mutants always showed reduced viability vs. controls. Statistical analysis was performed in BioConductor (Gentleman et al., 2004).

Results and discussion

Generation of mnn1 mutants

The *mnn1* locus is tightly flanked upstream by the *milton* gene (*milt*) and the *CG31907* gene is nested in a *mnn1* intron (Fig. 2A). Previously identified deletion alleles of *mnn1* (Busygina

et al., 2004;Papaconstantinou et al., 2005) are likely to disrupt the function of flanking genes in addition to *mnn1* (Fig. 2A). The $mnn1^{e200}$ allele is also mutant for *milt* (Busygina et al., 2004). The $mnn1^{e173}$ allele potentially disrupts *milt*. Both $mnn1^{e173}$ and $mnn1^{e30}$ delete sequences that approach the 3′ end of *CG31907* (Papaconstantinou et al., 2005). We have mobilized a P-element, $P\{wHy\}^{30G01}$, inserted in the 5′UTR of the *mnn1* locus (Fig. 2A), and screened for small deletions in order to identify new alleles of *mnn1* that would not affect other genes.

FlyBase (2003) annotates two *mnn1* transcripts, but neither of these transcripts have been isolated in previous molecular studies of the *mnn1* locus (Guru et al., 2001; Maruyama et al., 2000). Maruyama and Guru, independently, describe *mnn1* transcripts that differ from the two FlyBase annotations in the UTRs and in the terminal coding exon (Fig. 2B). A developmental profile of *mnn1* expression has revealed two *mnn1* transcripts (Guru et al., 2001) that are due to alternative poly-A sites (Fig. 2B). The shorter transcript annotated in FlyBase (*mnn1-RB*) may have been primed from an A-rich sequence in the intron of an unprocessed message rather than from the poly-A tail. Additionally, none of the 18 amino acids specific to Mnn1-PB are present in each of *mnn1* genes of the *Drosophila* species that we have reported in Fig. 1. Thus, the Muruyama and Guru gene models are our reference throughout this manuscript.

We generated two deletion alleles, $mnn1^{\Delta 46}$ and $mnn1^{\Delta 79}$. RT-PCR and sequence analysis indicate that the $mnn1^{\Delta 46}$ allele has a deletion of 573 bp of the *mnn1* locus missing 70 bp downstream of the first ATG of the *mnn1* ORF (Agarwal et al., 2004), while the $mnn1^{\Delta 79}$ allele has a more extensive deletion of 186 bp downstream of the start codon (Fig. 2B). However, all distal genes appeared to be intact, including CG31907 which is nested in *mnn1* intron 4. A third new allele, $Df(2L)mnn1^{\Delta 65}$ deletes at least 14 kb proximal to the 3′ end of the Muruyama and Guru *mnn1* gene model (Fig. 2B). This deletion, along with Df(2L)JH, removes several additional complementation groups required for viability (Fig. 2A).

Flies homozygous for either $mnn1^{\Delta 46}$ or $mnn1^{\Delta 79}$ are viable and fertile and can be readily maintained as homozygous stocks. Hemizygous $mnn1^{\Delta 46}$ or $mnn1^{\Delta 79}$ flies are also viable and fertile over Df(2L)mnn1 or Df(2L)JH. In addition to the mutant alleles, we selected two precise excision lines, $mnn1^{+84}$ and $mnn1^{+113}$, as wild type isogenic controls for further experiments. The $mnn1^{\Delta 46}$ and $mnn1^{\Delta 79}$ chromosomes were extensively backcrossed to control $y^{-}\ w^{-}$ flies to remove any undetected mutations associated with transposon mobilization.

Mnn1 mRNA isoforms are expressed in wild type early embryos and in adult females. The longer isoform is detected throughout development (Guru et al., 2001). To determine if the deletion alleles express *mnn1* mRNA, as might be expected given the presence of residual promoter region and upstream sequences, we performed RT-PCR reactions on total RNA extracts from $mnn1^{\Delta 46}$ to $mnn1^{\Delta 79}$ homozygous adult females and on perfect excision lines using multiple primer pairs also overlapping the ATG sequence and spanning *mnn1* intronic sequences (Fig. 2B, additional data not shown). The use of intron-spanning primers in the absence of reverse transcriptase allowed us to distinguish between transcripts and any contaminating genomic DNA. RT-PCR results obtained on wild type flies supported the first exon structure in the Muruyama and Guru gene model (Fig. 2D, additional data not shown). While no transcripts were detected with primers directed against deleted sequence in homozygous $mnn1^{\Delta 46}$ and $mnn1^{\Delta 79}$, transcripts were detected using primers downstream from those deletions (Fig. 2D). These results indicate that *mnn1* mRNAs are produced from the mutant alleles.

Both $mnn1^{\Delta 46}$ and $mnn1^{\Delta 79}$ alleles delete *mnn1* sequence coding for residues homologous to those known to be required for menin function in humans (Agarwal et al., 2004). In both $mnn1^{\Delta 46}$ or $mnn1^{\Delta 79}$, the first two in-frame ATGs of *mnn1* are deleted, such that homologs of

at least five amino acids required to prevent disease in humans are deleted due to a downstream translational start site utilization (Fig. 2C). To determine if *mnn1*$^{\Delta 46}$ and *mnn1*$^{\Delta 79}$ alleles encode defective menin proteins initiated from downstream AUGs in the mutant mRNAs (Fig. 2C), we performed immunoblots (Fig. 2E) and cell staining experiments (Figs. 3A–D). While these putative mutant polypeptides would be missing critical Mnn1 residues, they might retain some function (wild type or even dominant negative). Mnn1 proteins initiated by alternative downstream AUGs present in *mnn1* mutant mRNAs should migrate faster on SDS-PAGE. Immunoblot analysis performed with an antibody produced against an epitope mapping in exon 4 (Fig. 2B) showed a species migrating at ~ 95 kDa in extracts from wild type flies and extracts from bacteria expressing *Drosophila* Mnn1, but not from homozygous *mnn1*$^{\Delta 46}$ or *mnn1*$^{\Delta 79}$ flies (Fig. 2E). These results indicate that the antibody recognizes wild type Mnn1. We have analyzed protein extracts of whole adult females or males, third instar larvae and Central Nervous System (CNS) from third instar larvae and in no case did we detect a shorter isoform. Thus, in *mnn1*$^{\Delta 46}$ or *mnn1*$^{\Delta 79}$ larvae or adults, there is no evidence of N-terminally truncated Mnn1 proteins. Western blot results therefore simultaneously confirm that the bands in the wild type lanes correspond to endogenous Mnn1, not a cross-reacting species of similar mobility, and that the deletion alleles encode undetectable levels of N-terminally deleted Mnn1 protein. We did observe an anonymous slower migrating band in some of the Western blots (Fig. 2E); however, it is difficult to envision how a protein with this mobility could be encoded by *mnn1*. This band is almost certainly due to a cross-reacting species. We conclude that the *mnn1*$^{\Delta 46}$ and *mnn1*$^{\Delta 79}$ alleles are protein nulls. Previously reported *mnn1* alleles are also likely to be protein nulls (Busygina etal.,2004; Papaconstantinouetal., 2005). In no case has *mnn1* been shown to be required for viability or fertility. All these data strongly suggest that *mnn1* is not an essential gene in Drosophila.

Human menin is a nuclear protein (Guru et al., 1998). The *Drosophila* Mnn1 protein has a potential nuclear localization signal (KRTRR) in the region corresponding to the NLS-2 of human menin (Guru et al., 2001). The *mnn1* gene is broadly expressed throughout development (Guru et al., 2001). As expected, we detected Mnn1 immunoreactivity in the nuclei of the central nervous system (Fig. 3B), and many other larval tissues of wild type flies. Such staining was absent in flies homozygous for *mnn1*$^{\Delta 46}$ or *mnn1*$^{\Delta 79}$ (Fig. 3A). The weak anti-Mnn1 staining of endogenous protein was enriched in the nucleus and showed sub nuclear localization (Figs. 3E–H). To further evaluate the cellular localization of Drosophila Mnn1, we detected over-expressed Mnn1 following induction of *UAS-mnn1* with any number of Gal4 drivers (e.g. AB1, 69B, How24, dilp2 and OK6). In all cases, over-expressed Mnn1 is nuclear (Figs. 3I–P, additional data not shown). This staining is robust, again suggesting that endogenous Mnn1 is not abundant. Over-expressed Mnn1 from *Drosophila* extracts also co-migrates with bacterially expressed Mnn1 at ~ 95 kDa (not shown). These data suggest that, like mammalian menin, *Drosophila* menin is nuclear.

mnn1 loss-of-function phenotype

Flies lacking *mnn1* are viable and fertile as also shown by others (Busygina et al., 2004; Papaconstantinou et al., 2005). Our mutants show no overt and consistent phenotype as homozygote, trans-heterozygote or in trans to *Df(2L)mnn1*$^{\Delta 65}$ or Df(2L)J–H. As expected for a protein null allele, they behave as genetic amorphs, with the amorphic condition being viable, fertile, with no visible phenotype. *Mnn1*^{e200} flies were stated to have a reduced life span (Busygina et al., 2004). The *mnn1*^{e200} allele is deleted for both *mnn1* and *milt* (Fig. 2A), and the *milt* locus is required for viability. Thus, incomplete rescue with a *milt*$^{+}$ transgene could cause a reduction in life span (Busygina et al., 2004). However, our observations support the idea that *mnn1* is required for a wild type life span (Fig. 4A). A slight, but highly significant reduction in viability was observed both in homozygous *mnn1*$^{-}$ flies and in the trans-allelic *mnn1*$^{-}$ flies ($D = 0.35$, $P < 3 \times 10^{-4}$ by two-sample Kolmogorov–Smirnov test). There were

no significant differences between different genotypes of *mnn1*$^{-}$ ($P > 0.99$). Interestingly, the reduction in viability was due to a constant rate of early mortality of *mnn1*$^{-}$ males in days 1–30 ($D = 0.65$, $P < 2 \times 10^{-7}$ by two-sample Kolmogorov–Smirnov test).

It has also been reported that *mnn1*^{e173} and *mnn1*^{e30} mutants are sensitive to a range of stressors (Papaconstantinou et al., 2005), but again the results obtained might have been confounded by the more extensive deletions (Fig. 2A). We tested our *mnn1* mutant alleles for oxidative stress sensitivity using the herbicide paraquat, a powerful generator of reactive oxygen species. We find that flies either homozygous for the *mnn1*$^{-}$ alleles or trans-heterozygous for those alleles appear to be slightly more resistant to paraquat than *mnn1*$^{+}$ or *mnn1*$^{+}$/*mnn1*$^{-}$ flies ($D = 0.35$, $P < 3 \times 10^{-4}$ by two-sample Kolmogorov–Smirnov test) (Fig. 4B). This observation is more striking given the increased mortality of young *mnn1*$^{-}$ flies. Our results appear to be in contrast to what was reported previously by Papaconstantinou indicating that *mnn1*^{e178} or *mnn1*^{e30} flies are more sensitive to paraquat, not resistant. Determining if this inconsistency is due to the different nature of the generated mutants will require further investigation. The salient agreement among all the *mnn1* functional studies is that *mnn1* is a non-essential gene in *Drosophila*. The lack of a developmental defect in the more streamlined *Drosophila* genome is surprising as mice homozygous for *menin* null alleles die as embryos (Crabtree et al., 2001). There are no obvious additional *mnn1*-like genes in *Drosophila* suggesting that the absence of a developmental defect is not due to the function of a second *mnn1* gene. Perhaps menin has acquired non-conditional function only in the vertebrate lineage.

mnn1 over-expression phenotypes

We explored the consequences of excess *mnn1* expression by generating transgenic lines bearing the full-length *mnn1*$^{+}$ cDNA under the control of the yeast Gal4 inducible UAS promoter and a wide range of Gal4 drivers. It has been reported that uniform over-expression of Mnn1 does not alter development or viability (Papaconstantinou et al., 2005). We see distinct and dramatic effects of Mnn1 over-expression in a subset of tissues.

To begin systematically exploring the effect of Mnn1 over-expression on *Drosophila* development, we drove *mnn1* expression with Gal4 in a series of distinct spatiotemporal patterns (Table 1). Because the distribution of endogenous Mnn1 is quite broad, this is likely to increase the levels of Mnn1 in cells (cf. Figs. 3I–P), rather than altering the spatial distribution of Mnn1. The over-expression of Mnn1 protein (as determined by cell staining and/or immunoblotting) with any of five different Gal4 drivers (Table 1) resulted in a adult-pharate lethal phenotype (Figs. 5B–D). Interestingly, we found that all of these drivers are expressed in subsets of neurons in addition to the reported expression patterns. Development was arrested during late pupal morphogenesis at stage P14. Dissection of dead pupae shows deletion of distal elements of the proboscis and a melanotic mass at that location. The melanotic mass is evident prior to lethality (stage P7) as shown in Fig. 5C. Exceptional flies that escape adult-pharate lethality when *UAS-mnn1* is driven by How24-GAL4 (~ 5%) or 69B-GAL4 (~ 25%) show a melanotic mass at the anterior proboscis following eclosion. In the rare eclosing flies, the presence of a proboscis defect is not compatible with adult life, flies die 2–3 days later probably because of hindered intake of food and water. Wing inflation also failed in these escaping flies. Experiments performed at a lower temperature (22°) show an increased percentage of escaped flies and a reduced severity in the proboscis and wing defects. Gal4 is known to be less active at lower temperatures (Duffy, 2002), suggesting that the level of Mnn1 induction correlates with the intensity of the phenotype observed.

We occasionally observed a cleft thorax phenotype in flies when *UAS-mnn1* is driven with *69B-GAL4*. To further investigate the role of *mnn1* in the developing *Drosophila* thorax, we expressed *UAS-mnn1* using the *pnr-GAL4* driver, which is expressed specifically in the leading edge cells of the wing disc and the medial region of the thorax in adults (Calleja et al., 1996).

These cells participate in thorax closure during metamorphosis. Mnn1 protein is expressed throughout the wing disc in wild type flies and is clearly over-expressed in the leading edge cells in *pnr > mnn1* (not shown). The thorax of adult flies carrying one copy each of both *pnr-GAL4* and the *UAS-mnn1* transgene always showed a dorsal cleft along the entire thorax with disrupted chaetae orientation (Figs. 6B, D) whereas the thorax of flies carrying either one copy of *pnr-GAL4* or one copy of *UAS-mnn1* alone was wild type (Figs. 6A, C). This thoracic defect was 100% penetrant. Furthermore, the severity of the phenotype was modulated by the number of copies of *UAS-mnn1* expressed in the thorax (more copies result in a more extreme phenotype) and by the growth temperature, indicating that the phenotype is proportional to the degree of Mnn1 over expression (data not shown).

The cleft thorax phenotype raises the possibility that *Drosophila menin* can act in the *jun/fos* pathway. Thorax formation occurs by fusion of hemithoraces during pupal development as the result of spreading and fusion of two lateral groups of cells in the midline. This event requires the coordinated action of the Jun/Fos signaling pathway. Too little or too much Jun/Fos activity results in failure to properly suture imaginal discs during metamorphosis (Agnes et al., 1999; Martin-Blanco et al., 2000). Jun/Fos activity is also required for embryonic dorsal closure, but we never observed an overt dorsal closure phenotype associated with loss-of-function or over expression of *mnn1*. The latter may be due in part to the abundant maternally deposited *mnn1* transcript in embryos (Guru et al., 2001).

jun/fos interactions with mnn1 in the thorax

The cleft thorax phenotype is consistent with the idea that Mnn1 interacts with Jun/Fos, although this does not imply that the only function of *mnn1* is in the *jun/fos* pathway. We tested the idea of Mnn1 interacting with Jun/Fos by using an extensive set of crosses designed to explore genetic interactions between *mnn1* over-expressed with *pnr-GAL4* and jun/fos alleles (Figs. 6E–I). We over expressed Mnn1 in a heterozygous *jun* background (*jra*^{1}/+) and observed a more severe thoracic cleft phenotype. Similarly, the contextual over-expression of a dominant-negative *jun* (*UAS-jun*^{bZIP}) and *mnn1* enhanced the thorax defect. We also tested for an effect of the induction of *UAS-jun*^{bZIP} on the adult-pharate lethal phenotype observed in *How24 > mnn1* flies. While flies over-expressing *UAS-jun*^{bZIP} were wild type (Table 2), the flies expressing both *mnn1* and *jun*^{bZIP} showed a much earlier arrest of the pupal development (Fig. 5E), rather than the adult-pharate phenotype seen when only *mnn1* was over-expressed (Fig. 5D), again indicating that *mnn1* over-expression is exacerbated by dominant negative *jun* activity.

The synergistic effect of *mnn1* transgene and dominant negative alleles of *jun* along with the effect of altered *jun* dose suggests that menin acts to antagonize Jun protein function. If this is the case, then menin might suppress the effect of excess Jun activity. Expression of constitutively active, phosphomimetic *jun* (*UAS-jun*^{asp}) using *pnr-GAL4* results in fully penetrant embryonic lethality. In contrast, the simultaneous expression of *UAS-jun*^{asp} and *UAS-mnn1* driven from *pnr-GAL4* results in 1–5% of flies escaping to eclosion (Table 2). Thus, expression of Mnn1 suppresses the lethality associated with constitutive expression of active Jun. These data are consistent with *mnn1* acting as a negative regulator of *jun* function.

As *mnn1* shows a genetic interaction with *jun*, we also tested for interaction with *fos* (*kay*), the other component of the heterodimer. Heterozygosity for *kay*^{1} had no effect on the *mnn1* over-expression phenotype. However, expression of *UAS-fos* from *pnr-GAL4* results in a weak cleft thorax phenotype and this phenotype is greatly enhanced by simultaneous expression from *UAS-mnn1* (Table 2). Thus, excessive Fos is deleterious to Jun/Fos function, perhaps by affecting the homodimer/heterodimer ratio. These data suggest that menin and Fos have a negative synergistic effect on Jun/Fos function. However, genetic interactions between loss-of-function *mnn1* alleles and dominant-negative alleles of *fos* suggest that the interaction is

complex. In *mnn1*$^{-}$/*mnn1*$^{+}$ flies, over-expression of *fos*^{bZIP} with the *How24* driver has a more dramatic effect on thorax closure (Figs. 6J, K), and in the complete absence of *mnn1*, *How24-GAL4* induction of *fos*^{bZIP} results in pupal lethality (Table 2). Thus, in some experiments, Mnn1 is behaving as a positive regulator of Jun/Fos and in other experiments Mnn1 is acting as a negative regulator of Jun/Fos.

We also tested for dominant interactions between *mnn1* over-expression and loss-of-function alleles of other members of the Jun kinase (JNK) cascade, *hemipterous* (*hep*) or *basket* (*bsk*), that lead to activated Jun and the negative regulator *puckered* (*puc*), but saw no interaction. We also examined the phenotypic effects of simultaneous over-expression of *mnn1* with *hep*, *bsk* or *puc* and observed no interaction. Thus, there is no evidence that the interaction between *mnn1* and *jun/fos* is mediated by these components of the JNK signaling pathway. However, this does not imply that there is direct contact between Mnn1 and Jun/Fos proteins, and indeed, direct testing for physical interaction between Mnn1 and *Drosophila* Jun or Fos has revealed no interaction (Guru et al., 2001; and data not shown).

jun/fos interactions with mnn1 in eye development

Jun/Fos is also required for *Drosophila* eye morphogenesis (Kockel et al., 2001). Analysis of interactions between Mnn1 and Fos in eye development also suggests that Mnn1 can negatively or positively modulate Jun/Fos. While we observed no effect of *mnn1* over-expression in otherwise wild type eyes (Table 1), we did observe an interaction with Fos. Over-expression of a *fos* dominant negative, *UAS-fos*^{bZIP}, in the eye using *ey-GAL4* results in a small rough eye phenotype (Fig. 7B). The simultaneous induction of *mnn1* expression dramatically suppresses this severe small eye phenotype (Fig. 7C). Thus, even though loss-of-function and gain-of function of *mnn1* are not overtly deleterious to eye development, interaction with dominant negative *fos* reveals a genetic interaction of *mnn1* with *Jun/Fos* in the eye. Thus, wild type Mnn1 appears to augment Jun/Fos activity in the eye, or to negatively regulate the dominant negative activity of Fos^{bZIP}.

If Mnn1 is a positive regulator of Jun/Fos in the eye, then it might also enhance the effect of constitutive active *jun* in that tissue. We found the opposite. Induction of *UAS-jun*^{asp} by *ey-GAL4* resulted in pre-pupae lethality, but this was partially rescued by contextual over-expression of Mnn1. Flies expressing both *UAS-jun*^{asp} and *UAS-mnn1* driven by *ey-GAL4* eclose (1%), suggesting that Mnn1 can inhibit active Jun/Fos.

Conclusions

Mnn1 is highly conserved in *Drosophila*. Our experiments show that over-expressed Mnn1 can functionally interact with either wild type or over-expressed Jun/Fos. Furthermore, the absence of Mnn1 also modulates the activity of over-expressed Fos. Interestingly, these interactions result in defects consistent with both positive and negative influences of Mnn1 on Jun/Fos. While these results are unsatisfying for placing Mnn1 squarely in a particular and invariant position in the Jun/Fos pathway, it is clear that Jun/Fos is differently regulated in the eye and thorax of Drosophila (Kockel et al., 2001). It is also clear that mammalian Menin can function as either a positive or negative regulator of Jun family members (Agarwal et al., 2003). We suggest that there are contextual influences that allow Mnn1 to be both an activator or suppressor of Jun/Fos in *Drosophila*. This context-dependent effect might also underlie the opposing tumor suppressing (Chandrasekharappa et al., 1997; Crabtree et al., 2001) and tumor promoting (Yokoyama et al., 2005) effects of menin in mammals. Finally, while we have seen strong interactions between *mnn1* and *jun/fos*, this does not rule out a role for *mnn1* in other nuclear events. Indeed, mammalian menin is in a complex which is involved in modifying the histones at a large number of genes (Hughes et al., 2004;Yokoyama et al., 2004) and a large number of transcription factors have been reported to physically contact menin (Agarwal et

al., 2004). Why such a broad biochemical activity is associated with such modest phenotypic effects is not well understood in mammals or in *Drosophila*. Perhaps Mnn1 has a more subtle role in fine tuning gene expression.

Acknowledgements

This research was supported by the Intramural Research Program of the NIH (NIDDK, NHGRI, NICHD and OD). We acknowledge our colleagues Virginia Boulais, Diego Caro, Sandra Farkas and Jamileh Jemison for technical assistance, and members of the MEN1 consortium at the NIH. We are also grateful to the *Drosophila* community and the Bloomington *Drosophila* Stock Center, for generously and expeditiously sharing strains. Finally, we thank the *Drosophila* sequencing projects for making data public prior to formal publication.

References

Agarwal SK, Guru SC, Heppner C, Erdos MR, Collins RM, Park SY, Saggar S, Chandrasekharappa SC, Collins FS, Spiegel AM, Marx SJ, Burns AL. Menin interacts with the AP1 transcription factor JunD and represses JunD-activated transcription. Cell 1999;96:143–152. [PubMed: 9989505]

Agarwal SK, Novotny EA, Crabtree JS, Weitzman JB, Yaniv M, Burns AL, Chandrasekharappa SC, Collins FS, Spiegel AM, Marx SJ. Transcription factor JunD, deprived of menin, switches from growth suppressor to growth promoter. Proc Natl Acad Sci U S A 2003;100:10770–10775. [PubMed: 12960363]

Agarwal SK, Lee Burns A, Sukhodolets KE, Kennedy PA, Obungu VH, Hickman AB, Mullendore ME, Whitten I, Skarulis MC, Simonds WF, Mateo C, Crabtree JS, Scacheri PC, Ji Y, Novotny EA, Garrett-Beal L, Ward JM, Libutti SK, Richard Alexander H, Cerrato A, Parisi MJ, Santa Anna AS, Oliver B, Chandrasekharappa SC, Collins FS, Spiegel AM, Marx SJ. Molecular pathology of the MEN1 gene. Ann N Y Acad Sci 2004;1014:189–198. [PubMed: 15153434]

Agnes F, Suzanne M, Noselli S. The *Drosophila* JNK pathway controls the morphogenesis of imaginal discs during metamorphosis. Development 1999;126:5453–5462. [PubMed: 10556069]

Benson DA, Karsch-Mizrachi I, Lipman DJ, Ostell J, Wheeler DL. GenBank. Nucleic Acids Res 2005;33:D34–D38. [PubMed: 15608212]

Brand AH, Perrimon N. Targeted gene expression as a means of altering cell fates and generating dominant phenotypes. Development 1993;118:401–415. [PubMed: 8223268]

Busygina V, Suphapeetiporn K, Marek LR, Stowers RS, Xu T, Bale AE. Hypermutability in a *Drosophila* model for multiple endocrine neoplasia type 1. Hum Mol Genet 2004;13:2399–2408. [PubMed: 15333582]

Calleja M, Moreno E, Pelaz S, Morata G. Visualization of gene expression in living adult *Drosophila*. Science 1996;274:252–255. [PubMed: 8824191]

Chandrasekharappa SC, Guru SC, Manickam P, Olufemi SE, Collins FS, Emmert-Buck MR, Debelenko LV, Zhuang Z, Lubensky IA, Liotta LA, Crabtree JS, Wang Y, Roe BA, Weisemann J, Boguski MS, Agarwal SK, Kester MB, Kim YS, Heppner C, Dong Q, Spiegel AM, Burns AL, Marx SJ. Positional cloning of the gene for multiple endocrine neoplasia-type 1. Science 1997;276:404–407. [PubMed: 9103196]

Crabtree JS, Scacheri PC, Ward JM, Garrett-Beal L, Emmert-Buck MR, Edgemon KA, Lorang D, Libutti SK, Chandrasekharappa SC, Marx SJ, Spiegel AM, Collins FS. A mouse model of multiple endocrine neoplasia, type 1, develops multiple endocrine tumors. Proc Natl Acad Sci U S A 2001;98:1118–1123. [PubMed: 11158604]

Crabtree JS, Scacheri PC, Ward JM, McNally SR, Swain GP, Montagna C, Hager JH, Hanahan D, Edlund H, Magnuson MA, Garrett-Beal L, Burns AL, Ried T, Chandrasekharappa SC, Marx SJ, Spiegel AM, Collins FS. Of mice and MEN1: insulinomas in a conditional mouse knockout. Mol Cell Biol 2003;23:6075–6085. [PubMed: 12917331]

Duffy JB. GAL4 system in *Drosophila*: a fly geneticist's Swiss army knife. Genesis 2002;34:1–15. [PubMed: 12324939]

FlyBase. The FlyBase database of the *Drosophila* genome projects and community literature. Nucleic Acids Res 2003;31:172–175. [PubMed: 12519974]

Gallo A, Cuozzo C, Esposito I, Maggiolini M, Bonofiglio D, Vivacqua A, Garramone M, Weiss C, Bohmann D, Musti AM. Menin uncouples Elk-1, JunD and c-Jun phosphorylation from MAP kinase activation. Oncogene 2002;21:6434–6445. [PubMed: 12226747]

Gentleman RC, Carey VJ, Bates DM, Bolstad B, Dettling M, Dudoit S, Ellis B, Gautier L, Ge Y, Gentry J, Hornik K, Hothorn T, Huber W, Iacus S, Irizarry R, Leisch F, Li C, Maechler M, Rossini AJ, Sawitzki G, Smith C, Smyth G, Tierney L, Yang JY, Zhang J. Bioconductor: open software development for computational biology and bioinformatics. Genome Biol 2004;5:R80. [PubMed: 15461798]

Gobl AE, Berg M, Lopez-Egido JR, Oberg K, Skogseid B, Westin G. Menin represses JunD-activated transcription by a histone deacety-lase-dependent mechanism. Biochim Biophys Acta 1999;1447:51–56. [PubMed: 10500243]

Goldsmith P, Gierschik P, Milligan G, Unson CG, Vinitsky R, Malech HL, Spiegel AM. Antibodies directed against synthetic peptides distinguish between GTP-binding proteins in neutrophil and brain. J Biol Chem 1987;262:14683–14688. [PubMed: 3117789]

Guru SC, Goldsmith PK, Burns AL, Marx SJ, Spiegel AM, Collins FS, Chandrasekharappa SC. Menin, the product of the MEN1 gene, is a nuclear protein. Proc Natl Acad Sci U S A 1998;95:1630–1634. [PubMed: 9465067]

Guru SC, Prasad NB, Shin EJ, Hemavathy K, Lu J, Ip YT, Agarwal SK, Marx SJ, Spiegel AM, Collins FS, Oliver B, Chandrasekharappa SC. Characterization of a MEN1 ortholog from *Drosophila melanogaster*. Gene 2001;263:31–38. [PubMed: 11223240]

Huet F, Lu JT, Myrick KV, Baugh LR, Crosby MA, Gelbart WM. A deletion-generator compound element allows deletion saturation analysis for genomewide phenotypic annotation. Proc Natl Acad Sci U S A 2002;99:9948–9953. [PubMed: 12096187]

Hughes CM, Rozenblatt-Rosen O, Milne TA, Copeland TD, Levine SS, Lee JC, Hayes DN, Shanmugam KS, Bhattacharjee A, Biondi CA, Kay GF, Hayward NK, Hess JL, Meyerson M. Menin associates with a trithorax family histone methyltransferase complex and with the hoxc8 locus. Mol Cell 2004;13:587–597. [PubMed: 14992727]

Karnik SK, Hughes CM, Gu X, Rozenblatt-Rosen O, McLean GW, Xiong Y, Meyerson M, Kim SK. Menin regulates pancreatic islet growth by promoting histone methylation and expression of genes encoding p27Kip1 and p18INK4c. Proc Natl Acad Sci U S A 2005;102:14659–14664. [PubMed: 16195383]

Kim H, Lee JE, Kim BY, Cho EJ, Kim ST, Youn HD. Menin represses JunD transcriptional activity in protein kinase Ctheta-mediated Nur77 expression. Exp Mol Med 2005;37:466–475. [PubMed: 16264271]

Knapp JI, Heppner C, Hickman AB, Burns AL, Chandrasekharappa SC, Collins FS, Marx SJ, Spiegel AM, Agarwal SK. Identification and characterization of JunD missense mutants that lack menin binding. Oncogene 2000;19:4706–4712. [PubMed: 11032020]

Kockel L, Homsy JG, Bohmann D. *Drosophila* AP-1: lessons from an invertebrate. Oncogene 2001;20:2347–2364. [PubMed: 11402332]

Martin-Blanco E, Pastor-Pareja JC, Garcia-Bellido A. JNK and decapentaplegic signaling control adhesiveness and cytoskeleton dynamics during thorax closure in *Drosophila*. Proc Natl Acad Sci U S A 2000;97:7888–7893. [PubMed: 10884420]

Maruyama K, Tsukada T, Honda M, Nara-Ashizawa N, Noguchi K, Cheng J, Ohkura N, Sasaki K, Yamaguchi K. Complementary DNA structure and genomic organization of *Drosophila* menin. Mol Cell Endocrinol 2000;168:135–140. [PubMed: 11064160]

Mechta-Grigoriou F, Gerald D, Yaniv M. The mammalian Jun proteins: redundancy and specificity. Oncogene 2001;20:2378–2389. [PubMed: 11402334]

Milne TA, Hughes CM, Lloyd R, Yang Z, Rozenblatt-Rosen O, Dou Y, Schnepp RW, Krankel C, Livolsi VA, Gibbs D, Hua X, Roeder RG, Meyerson M, Hess JL. Menin and MLL cooperatively regulate expression of cyclin-dependent kinase inhibitors. Proc Natl Acad Sci U S A 2005;102:749–754. [PubMed: 15640349]

Naito J, Kaji H, Sowa H, Hendy GN, Sugimoto T, Chihara K. Menin suppresses osteoblast differentiation by antagonizing the AP-1 factor, JunD. J Biol Chem 2005;280:4785–4791. [PubMed: 15563473]

Papaconstantinou M, Wu Y, Pretorius HN, Singh N, Gianfelice G, Tanguay RM, Campos AR, Bedard PA. Menin is a regulator of the stress response in *Drosophila melanogaster*. Mol Cell Biol 2005;25:9960–9972. [PubMed: 16260610]

Rubin GM, Spradling AC. Genetic transformation of *Drosophila* with transposable element vectors. Science 1982;218:348–353. [PubMed: 6289436]

Scacheri PC, Crabtree JS, Kennedy AL, Swain GP, Ward JM, Marx SJ, Spiegel AM, Collins FS. Homozygous loss of menin is well tolerated in liver, a tissue not affected in MEN1. Mamm Genome 2004;15:872–877. [PubMed: 15672591]

Tateno M, Nishida Y, Adachi-Yamada T. Regulation of JNK by Src during *Drosophila* development. Science 2000;287:324–327. [PubMed: 10634792]

Yokoyama A, Wang Z, Wysocka J, Sanyal M, Aufiero DJ, Kitabayashi I, Herr W, Cleary ML. Leukemia proto-oncoprotein MLL forms a SET1-like histone methyltransferase complex with menin to regulate Hox gene expression. Mol Cell Biol 2004;24:5639–5649. [PubMed: 15199122]

Yokoyama A, Somervaille TC, Smith KS, Rozenblatt-Rosen O, Meyerson M, Cleary ML. The menin tumor suppressor protein is an essential oncogenic cofactor for MLL-associated leukemogenesis. Cell 2005;123:207–218. [PubMed: 16239140]

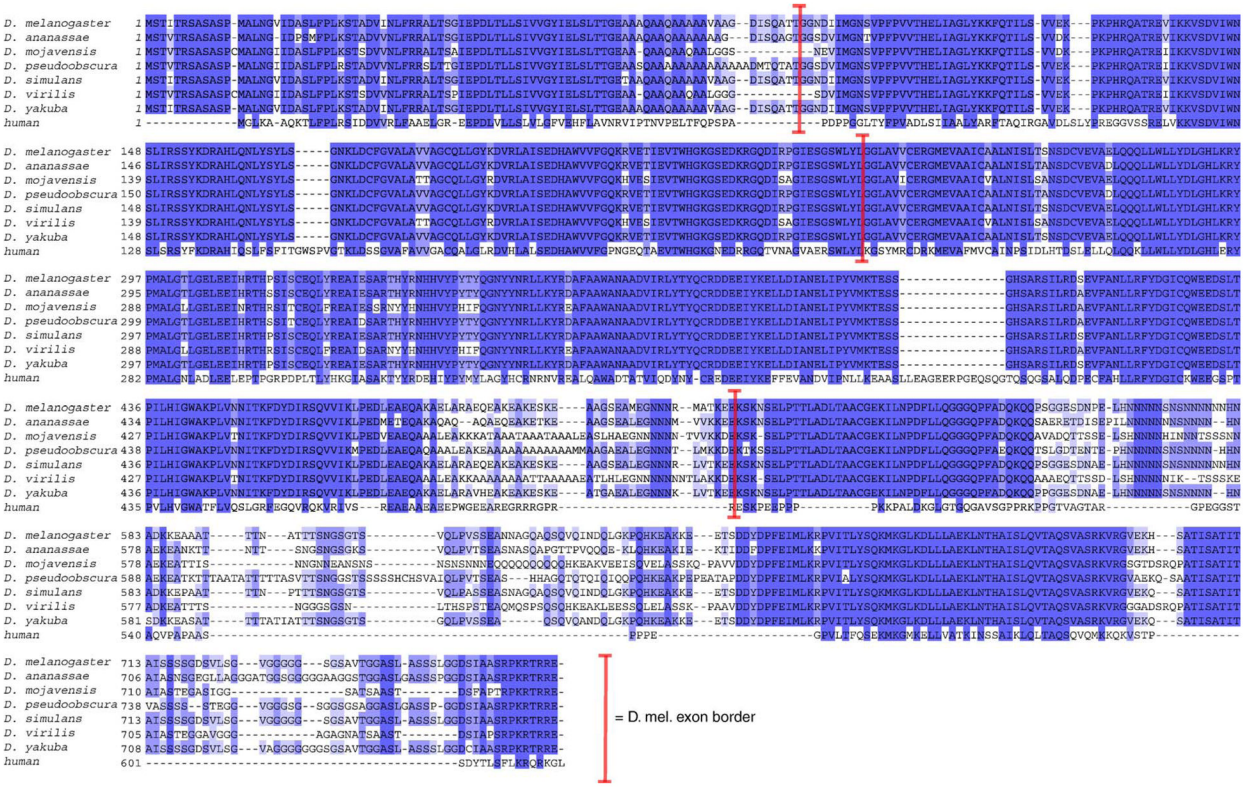

Fig. 1.

Alignment of predicted menin polypeptides in *Drosophila* species. Multiple alignment of predicted menin protein sequences from seven species of *Drosophila* compared to human performed by ClustalW. Conserved residues (shaded) and *Drosophila melnaogaster* splice junctions (brackets). Human (gi|18860839, NP_000235.2) and *Drosophila melanogaster* (gi: 28574051, NP_523498.2) sequences are from Genbank (Benson et al., 2005). *Drosophila pseudoobscura* sequence is from FlyBase (FlyBase, 2003). Remaining sequences are from draft annotations (V. N. Iyer, D. A. Pollard and M. B. Eisen, personal communication) of assemblies generated by Agencourt (D. Smith, personal communication) and Washington University (R. Wilson, personal communication) genome sequencing centers.

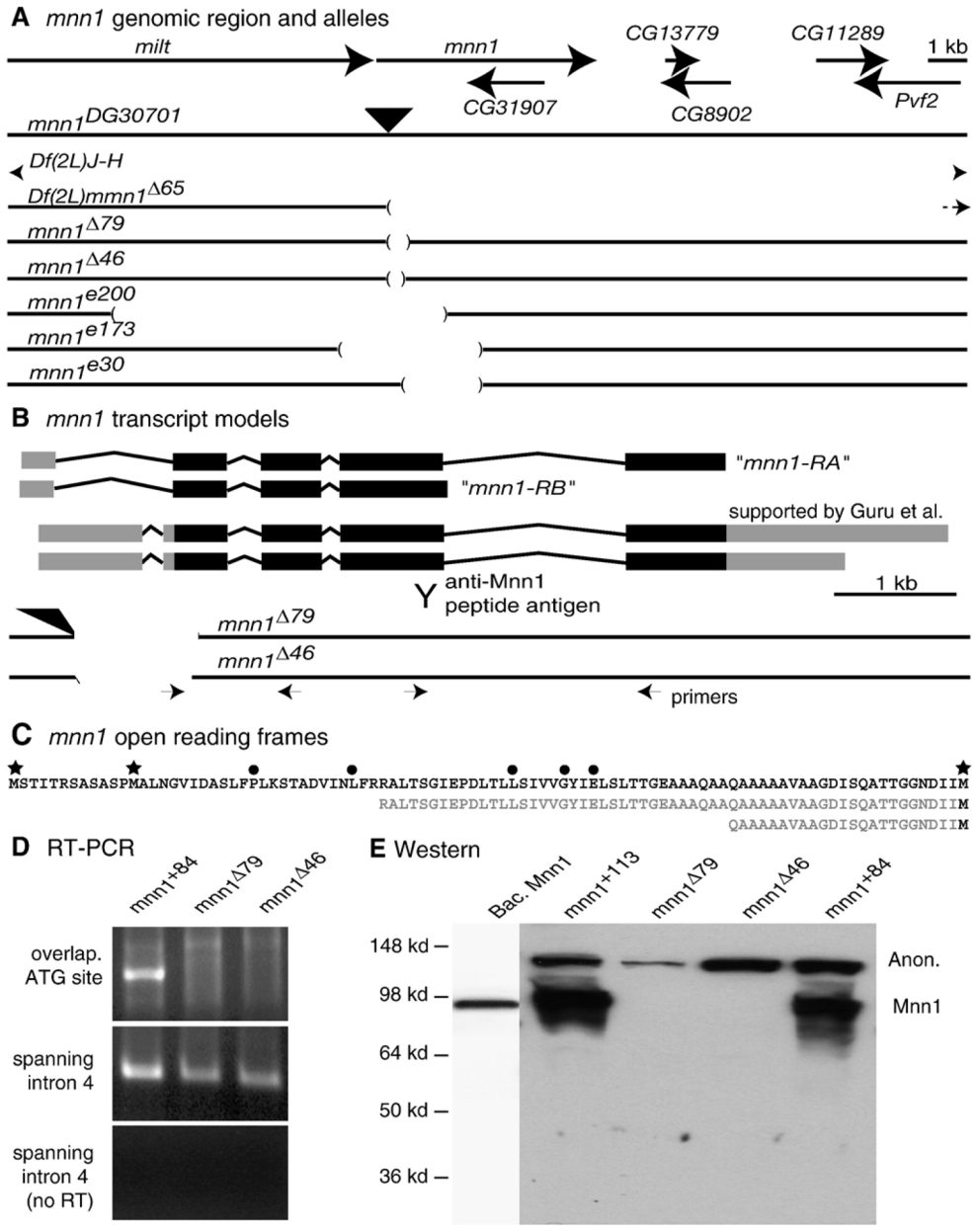

Fig. 2.

Map of mnn1 locus and description of mnn1 alleles. (A) Molecular map of the *mnn1* genomic region showing the flanking gene *milton* (*milt*) and the CG31907 gene nested in *mnn1*. Big arrows indicate the 5′ to 3′ orientation of the genes. Genomic maps of *mnn1* mutants are reported in scale below. The black filled triangle localizes the $P\{wHy\}^{30G01}$ insertion. Gaps in lines indicate the deleted genomic sequences described for each *mnn1* mutant allele. (B) Molecular map of the *mnn1* transcripts. Filled boxes show exons, thin lines show introns, black filling indicates the open reading frame, gray filling indicates untranslated regions and alternative poly-A. Mnn1-RA and mnn1-RB indicate the long and the short transcript annotated in FlyBase. Y sign indicates the antigenic sequence used to generate anti-Mnn1. Interrupted lines show genomic map of $mnn1^{\Delta 46}$ and $mnn1^{\Delta 79}$ alleles in scale with the *mnn1* transcripts. Small arrows localize the sites and directions of RT-PCR primers. (C) Amino acid sequence of N-

terminus of Mnn1 protein. Stars indicate alternative translational start sites. Filled circles indicate amino acid residues mutated in MEN1 patients. Sequences in gray show the amino acid residues missing in *mnn1*$^{\Delta 46}$ and *mnn1*$^{\Delta 79}$ due to the absence of the ATG (D) RT-PCR analysis of RNA extracted from *mnn1*$^{+84}$ precise-excision and *mnn1*$^{\Delta 46}$ and *mnn1*$^{\Delta 79}$ mutant strains, using a primer overlapping the ATG sequence (upper panel) or primers spanning intron 4 sequence (middle panel). Control for genomic DNA contamination is shown (lower panel). (E) Western blot anti-Mnn1 on bacterial expressed pure Mnn1 and protein extracts from wild type (*mnn1*$^{+113}$ and *mnn1*$^{+84}$) and *mnn1* mutant (*mnn1*$^{\Delta 46}$ and *mnn1*$^{\Delta 79}$) adult heads. All lanes are from a single blot. Expected mobility of Mnn1 and an anonymous (Anon) cross-reacting material is shown.

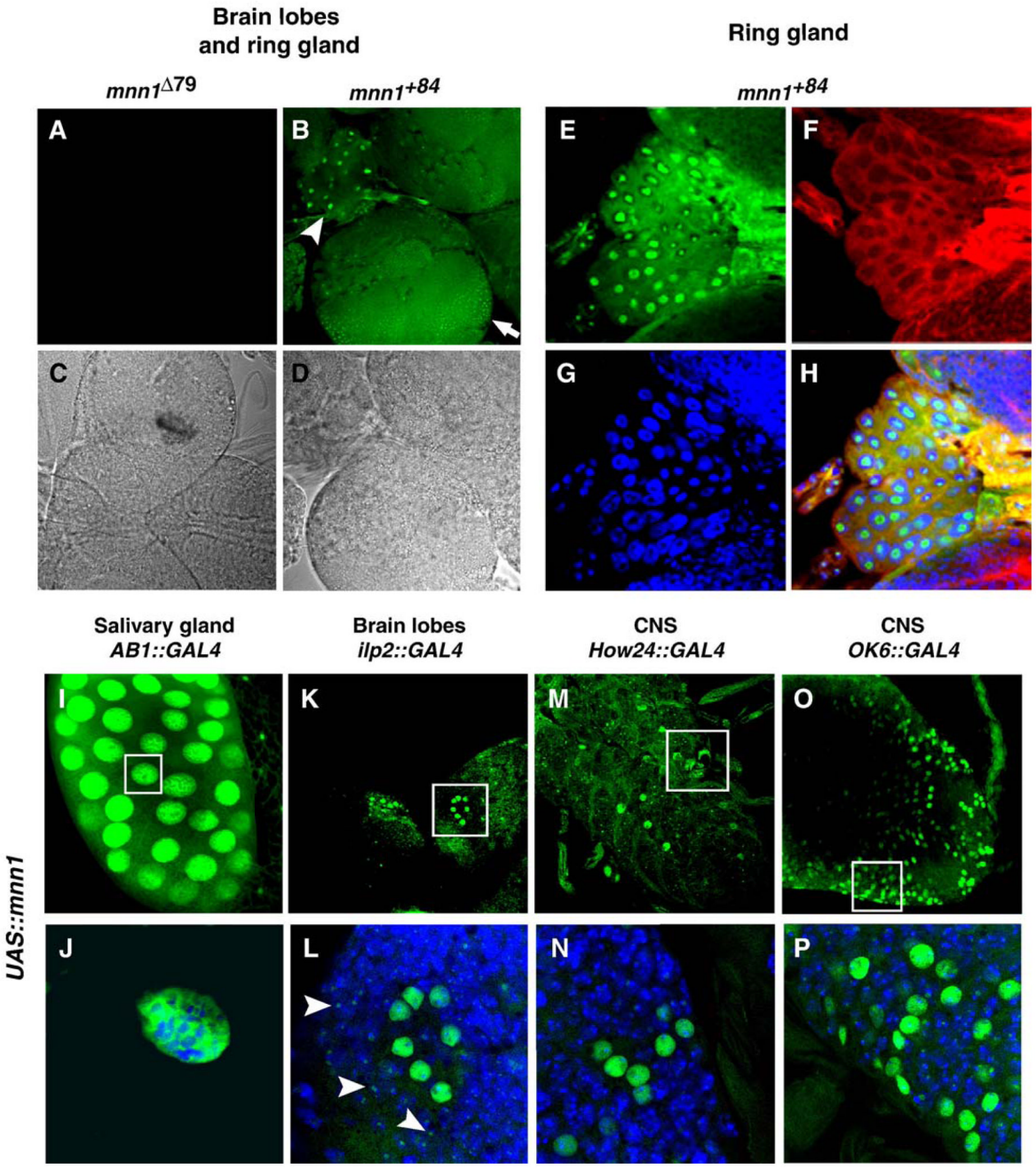

Fig. 3.

Anti-Mnn1 tissue staining in wild type, over-expressing and Mnn1 null mutants. (A–D) Anti-Mnn1 immunofluorescence (green) of third instar larval brain, in wild type (B, D) and protein null (A, C). Immunofluorescent (A, B) and differential contrast channels (C, D) of the same preparation are shown. Staining is observed in the brain hemispheres (arrow) and ring gland (arrow head). (E–H) Multiple channel view of magnified ring gland polyploid tissue. Mnn1 is stained in green (E), actin in red (F) and DNA in blue (G). Merge of the three channels (H) reveals weak but consistent nuclear staining of Mnn1. Nuclear staining appears non-uniform. (I–P) Mnn1 staining (green) in third instar larvae following *UAS-mnn1* induction by *AB1-GAL4* driver in salivary gland (I), insulin *dilp2-GAL4* driver in brain lobe (K), *How24-GAL4*

driver in CNS (M), motor neuron OK6-GAL4 driver in CNS (O). (J, L, N, P) Magnification of groups of cells showing intense Mnn1 staining (empty boxes in upper panel). Double staining for DNA (blue) clearly shows Mnn1 in the nucleus of polytene salivary cells (J) and nuclei of groups of neurons (L, N, P). Weaker Mnn1 staining appears punctate (arrowheads in panel L) and may represent endogenous Mnn1 in surrounding cells.

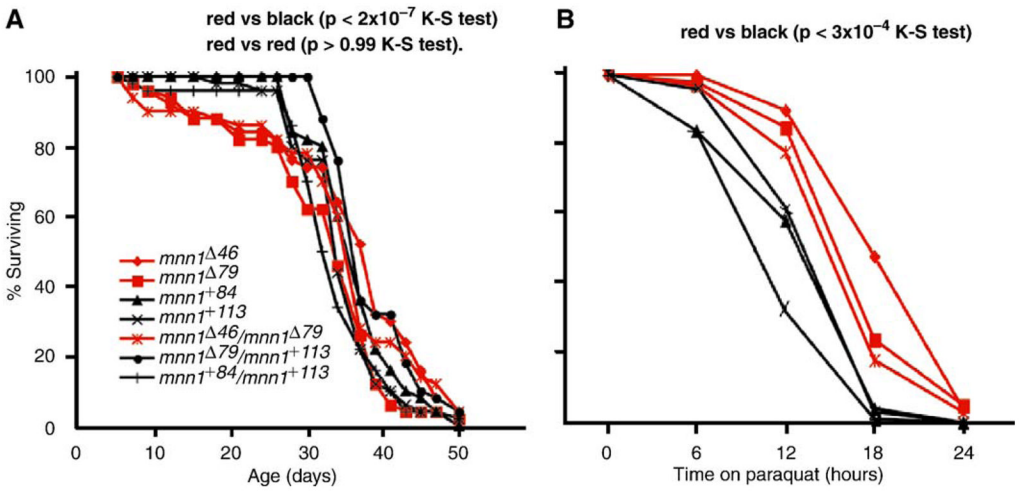

Fig. 4.

Loss-of-function *mnn1* phenotypes. Analysis of *mnn1*$^{-}$ mutant (red lines) and *mnn1*$^{+}$ control (black lines) for survival on standard media (A) and on 10 mM paraquat in sucrose (B). Genotypes are indicated. (A) Red vs. black lines show a significant survival difference ($P < 3 \times 10^{-4}$ K–S test) more evident in the first 30 days ($P < 2 \times 10^{-7}$ K–S test) while red vs. red lines are almost identical ($P > 0.99$ K–S test). (B) Red vs. black lines show a slight difference ($P < 3 \times 10^{-4}$ K–S test) in oxidative stress response.

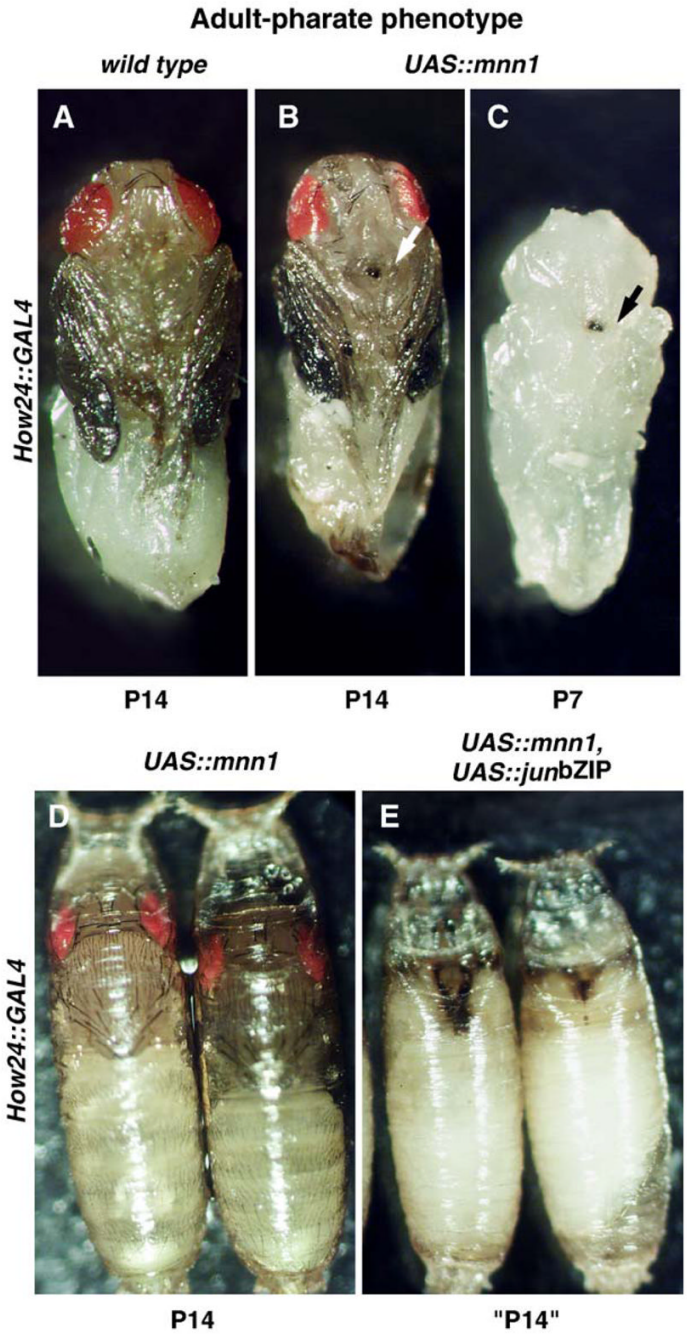

Fig. 5.

Over-expression of *mnn1* results in adult-pharate phenotype enhanced by jun dominant negative. (A) Wild type pupae dissected at developmental stage P14 corresponding to the time of death caused by *mnn1* induction. (B) Adult-pharate phenotype observed when *UAS-mnn1* is driven by *How24-GAL4*. Note the dark spot at the end of the proboscis (arrow). (C) The dark spot is detectable as early as pupal stage P7 (arrow), same genotype as panel B. (D) Pupae over-expressing *mnn1* die later than (E) pupae over-expressing *mnn1* and dominant negative *jun* contextually (*UAS-mnn1* and *UAS-jun*^{bZIP} driven by *How24-GAL4*).

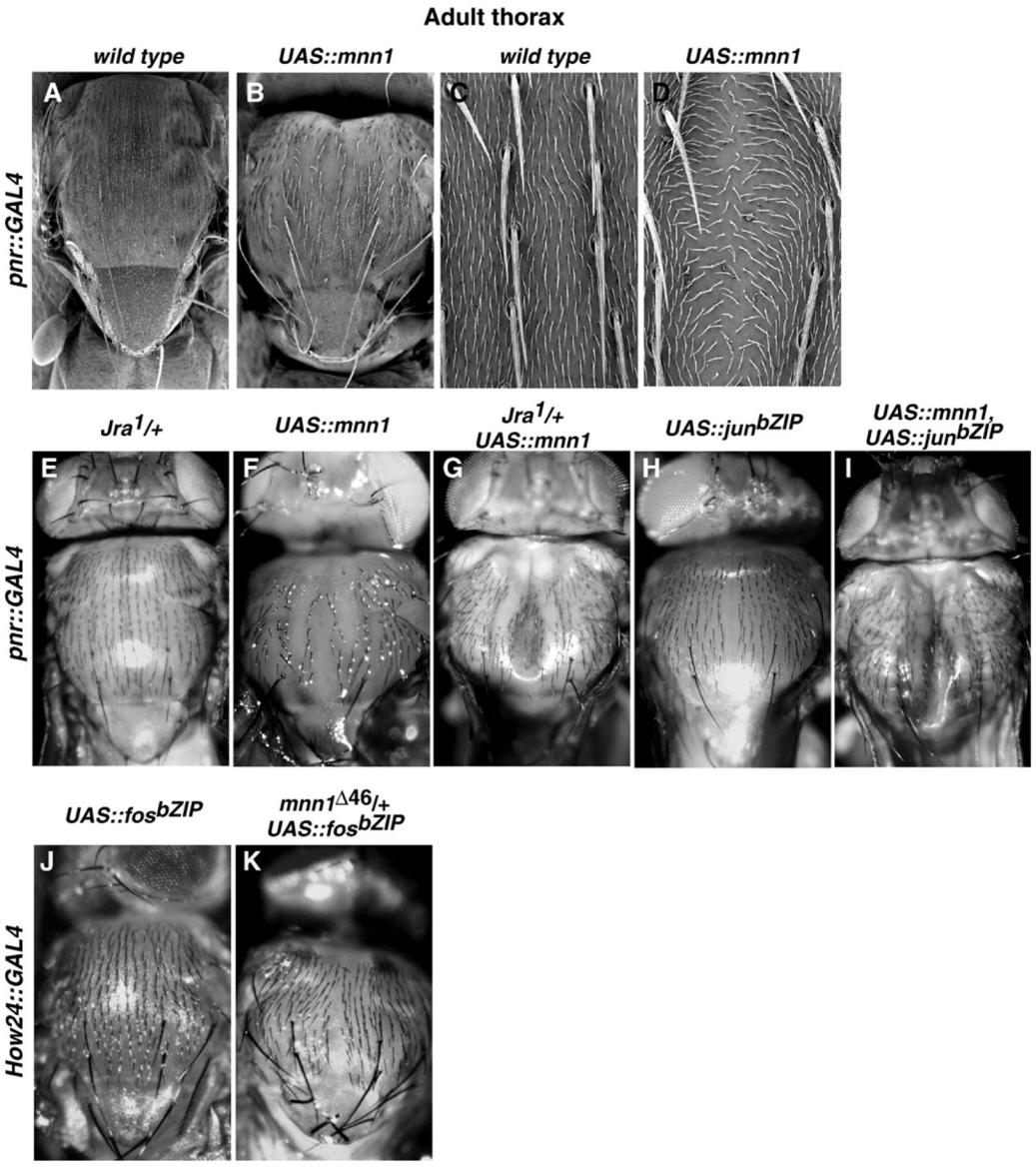

Fig. 6.

Thoracic over-expression of *mnn1* and interactions between Mnn1 and Jun/Fos in the thorax. (A) Dorsal view of thorax in wild type. (B) Dorsal view of thorax when *UAS-mnn1* is driven by *pnr-GAL4*. The thorax is reduced in the anterior–posterior dimension, the scutum is slightly enlarged, the scutellum is shortened, intrascutal and scutoscutellar sutures are less evident, scutellar bristles are curved and shorter. (D) SEM view of the thoracic dorsal midline showing an enlarged space between the dorsocentral bristles. (C) Wild type bristle distribution. (E) Absence of thoracic abnormalities in *Jun* defective flies (*jra*^{1}/+). (F) Thoracic defect observed when *UAS-mnn1* is driven by *pnr-GAL4* in the thorax. (G) Enhanced thoracic cleft in flies with reduced dose of *jun* and over-expressing *mnn1*. (H) Mild defect of thoracic closure produced by over-expression of a *jun* dominant-negative when *UAS-jun*$^{\mathrm{bZIP}}$ is driven by *pnr-GAL4*. (I) Enhanced thoracic cleft when *UAS-mnn1* and *UAS-jun*$^{\mathrm{bZIP}}$ are driven simultaneously by *pnr-GAL4*. (J) Absence of thoracic defect in flies over-expressing a dominant negative *fos* (*UAS-fos*$^{\mathrm{bZIP}}$) with the *How24* driver. (K) Moderate thoracic defect detected in eclosed flies

expressing *fos* dominant negative with reduced dose of *mnn1*. Absence of *mnn1* in *How24* > fos^{bZIP} flies results in pupae lethality (Table 2).

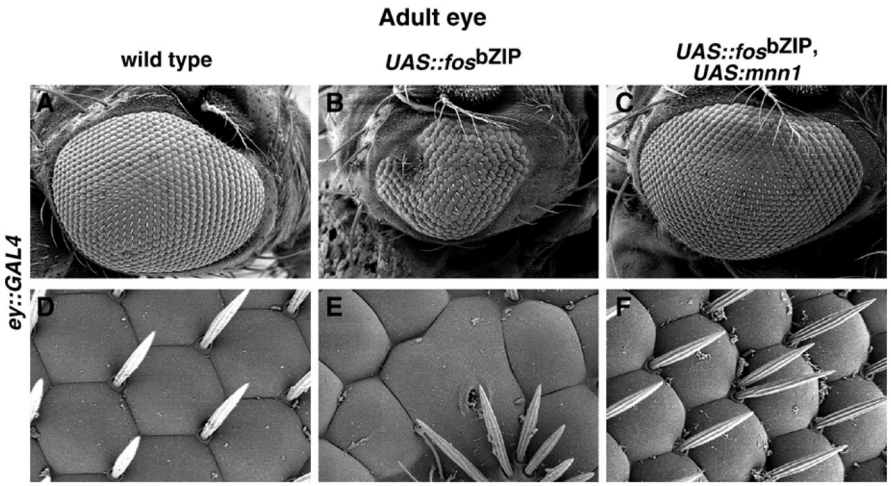

Fig. 7.

Interactions between Mnn1 and Fos in the eye. (A, D) Wild type eye showing the organization of normal ommatidia. (B, E) Small-rough eye phenotype resulting from the expression of *fos* dominant negative (*UAS-fos*^{bZIP} driven by the *ey-GAL4* driver). The number and hexagonal shape of ommatidia, as well as the distribution of the mechanical bristles are altered. (C, F) *Mnn1* over-expression reverts the phenotype when *UAS-mnn1* and *UAS-fos*^{bZIP} are driven by *ey-GAL4*. (A–C) × 125; (D–F) × 1000.

Table 1

UAS-mnn1 phenotypes induced by *Gal4* drivers

***Gal4* driver**	**Reported expression pattern** [a]	**Phenotype with *UAS-mnn1***
How24	Mesoderm[b]	Pharate lethal, cleft thorax
elav^{C155}	CNS	Pharate lethal
daG32^{UH1}	Ubiquitous	Pharate lethal
69B	Ectoderm[b]	Pharate lethal, cleft thorax
OK6	Motor neurons	Pharate lethal
twiG$^{108.4}$	Mesoderm	wt
ninaE.GMR^{12}	Morphogenic eye	wt
ey.H$^{3-8}$	Eye primordia	wt
C1003	Ectoderm, CNS	wt
AB1	Salivary gland	wt
crc929	Neuroendocrine	wt
dilp2	Insulin secreting neurons	wt
48Y	Endoderm	wt
dpp.blk1^{40C6}	dpp pattern	wt
pnr^{MD237}	pnr pattern	Cleft thorax

[a] See Flybase (2003) for references.

[b] Also expressed in a subset of neurons.

Table 2

Over-expression of *mnn1* in *jun* or *fos* backgrounds

***mnn1* genotype**	***jun* genotype**	***fos* genotype**	***pnr-GAL4* phenotype** [a]	***ey-GAL4* phenotype**	***How24-GAL4* phenotype**
	UAS-jun		wt	wt	wt
		UAS-fos	Weak cleft thorax (class I/II)	wt	wt
UAS-mnn1			Moderate cleft thorax (class II)	wt	Pharate lethal (P14)
UAS-mnn1		*UAS-fos*	Strong cleft thorax (class III/IV)	wt	Pharate lethal (P14)
UAS-mnn1	*UAS-jun*		Moderate cleft thorax (class II)	wt	Pharate lethal (P14)
	$jra^{1}/+$		wt	wt	wt
UAS-mnn1	$jra^{1}/+$		Strong cleft thorax (class III)	n.d.	n.d.
	$UAS\text{-}jun^{bZIP}$		Weak cleft thorax (class I)	wt	wt
UAS-mnn1	$UAS\text{-}jun^{bZIP}$		Cleft thorax (strong)	wt	Pupal lethal (P7)
	$UAS\text{-}jun^{asp}$		Lethal[b]	Lethal[b]	Lethal[b]
UAS-mnn1	$UAS\text{-}jun^{asp}$		Semi-lethal[c]	Semi-lethal[d]	Lethal
		$UAS\text{-}fos^{bZIP}$	Strong cleft thorax (class III)	Small rough eye	wt
UAS-mnn1		$UAS\text{-}fos^{bZIP}$	Strong cleft thorax (class III)	wt	Lethal
$mnn1^{\Delta 46}/+$		$UAS\text{-}fos^{bZIP}$	n.d.	n.d.	Moderate cleft thorax (class II)
$mnn1^{\Delta 46}/mnn1^{\Delta}79$		$UAS\text{-}fos^{bZIP}$	n.d.	n.d.	Pre-pupal lethal

[a] Description and classifications (Tateno et al., 2000) of thorax phenotypes are given.

[b] Fully penetrant lethality. Thorax and eye phenotypes unscorable.

[c] 5% eclosion. Viable flies have a severe cleft thorax (class IV).

[d] < 5% eclosion. Viable flies have small rough eyes.